Thermal and Mechanical Properties of Cross-Linked Photopolymers Based on Multifunctional Thiol−Urethane Ene Monomers

Askim F. Senyurt,[†] Charles E. Hoyle,*[,†] Huanyu Wei,[†] Scott G. Piland,[‡] and Trenton E. Gould[‡]

School of Polymers and High Performance Materials and School of Human Performance and Recreation, University of Southern Mississippi, 118 College Drive, Hattiesburg, Mississippi 39406

Received November 17, 2006; Revised Manuscript Received February 8, 2007

ABSTRACT: Urethane-based multiene monomers were synthesized and photopolymerized with a trifunctional thiol monomer to form highly cross-linked thiol−ene networks. Real-time FTIR was used to monitor the conversion of thiol and urethane ene monomers as a function of irradiation time. For stoichiometric thiol−urethane ene photopolymerizations, monomers reacted in a 1:1 molar functional group ratio, reaching ~90% monomer conversion within several seconds. The effects of the ene chemical structure and concentration on thermal and mechanical properties were characterized by DMA, DSC, TGA, tensile, and energy absorption upon nondestructive impact. The temperature at tan δ_{max} of the thiol−urethane ene networks was around 39 °C and decreased to lower temperatures with the addition of a reactive diluent diallyl ether ene monomer. Tensile and impact results were combined with fracture toughness measurements to elucidate the effect of the urethane and bisphenol A chemical structures. The energy absorption was dependent on the glass transition temperature of the thiol−urethane ene cross-linked networks. Improvement in fracture toughness and tensile properties was observed with the incorporation of 10 mol % of an ene with a bisphenol A structure. Scanning electron micrographs of fractured surfaces were used to interpret the nature of the brittle fracture. All of the properties of the thiol−urethane ene networks were compared to a conventional trithiol−triallyltriazine trione-based matrix.

Introduction

Photopolymerization is an efficient method for producing cross-linked materials with thicknesses ranging from a few microns to several millimeters. Traditional applications include offset lithography, dental and medical materials, and printing inks as well as protective films on floors, wood, compact discs, and optical fibers.[1,2] The solvent-free formulations, fast polymerization rates, and reduced energy consumption of photocuring make it attractive for numerous applications. A wide variety of monomers have been reported to undergo rapid polymerization when exposed to light in the presence of a photoinitiator. (Meth)-acrylate and thiol−ene monomers are prominent examples of efficient photopolymerizable monomers.

The photopolymerization of thiol and ene mixtures occurs by a free-radical chain mechanism involving a two-step propagation process. The free-radical step-growth process forms a uniform cross-linked network involving the addition of the thiyl radical to the ene double bond to yield a carbon-centered radical followed by the hydrogen abstraction of a thiol from the carbon-centered radical to regenerate a thiyl radical.[3−7] Thiol−ene polymerizations are known for proceeding with very little oxygen inhibition.[5,7] Other important characteristics of thiol−ene polymerization include delayed onset of the gel point compared to acrylates,[6] low shrinkage, and fast polymerization rates with high monomer conversions.[3−7] Multifunctional thiol monomers readily react with any monomer bearing multiple terminal double bond to form highly cross-linked matrices with varying material properties. However, because of the highly cross-linked nature of these materials, thiol−ene based polymers produced with off the shelf chemicals suffer from low elongations at break, insufficient fracture toughness, and poor tear strengths.[8]

Urethane chemistry utilizes the condensation reaction of isocyanates and alcohols to form a urethane (carbamate) structure.[9] Well-known applications of polyurethanes include thermoplastic elastomers, automotive parts, adhesives, rigid foams for insulation, and fibers.[9] High molecular weight oligomers of polyurethanes are prepared from the polyaddition reaction of diisocyanates with di- and tri-alcohols. Urethane groups form stable intermolecular hydrogen bonds between molecules which result in highly viscous materials.[9] Because of hydrogen bonding, urethane groups impart properties such as toughness, abrasion resistance, and high tear strength. Accordingly, polyurethanes exhibit a wide variety of property combinations depending on their exact composition. The inherent reactivity of diisocyanates also makes them useful for synthesis of reactive monomers with urethane bridging groups. Diisocyanates react with multifunctional alcohols in non-stoichiometric ratios to form isocyanate-terminated products that can be end-capped with functionalized monoalcohols to form functionalized urethane oligomers with reactive terminal double bonds.[9]

A key opportunity for thiol−ene systems is to simultaneously attain a network that exhibits high-energy absorption upon nondestructive impact, high elongation at break, excellent fracture toughness, and high tear strength. Such networks would be extremely valuable in a variety of athletic and other personnel protection applications where energy absorption under conditions where impact forces less than required to produce material failure are routinely encountered. Accordingly, herein we report the results of an initial work designed to demonstrate how the fracture toughness and nondestructive impact energy absorption of photocurable thiol−ene monomers are dramatically enhanced by a combination of urethane chemical architecture and free radical thiol−ene reactions. Two sets of ene monomers were

* To whom correspondence should be addressed: e-mail charles.hoyle@usm.edu; Ph 601-266-4873; Fax 601-266-5504.
[†] School of Polymers and High Performance Materials.
[‡] School of Human Performance and Recreation.

10.1021/ma0626463 CCC: $37.00
Published on Web 03/31/2007

Chart 1. Chemical Structures of (a) Isophorone Diisocyanate (IPDI), (b) 4,4′-Methylenebis(cyclohexyl isocyanate) (H_{12}MDI), (c) Toluene Diisocyanate (TDI), (d) Triallyloxytriazine (TAOT), (e) Bisphenol A Propoxylate (BPAP), (f) Trimethylolpropane Diallyl Ether (DAE), and (g) Trimethylolpropane Tris(3-mercaptopropionate) (TriThiol)

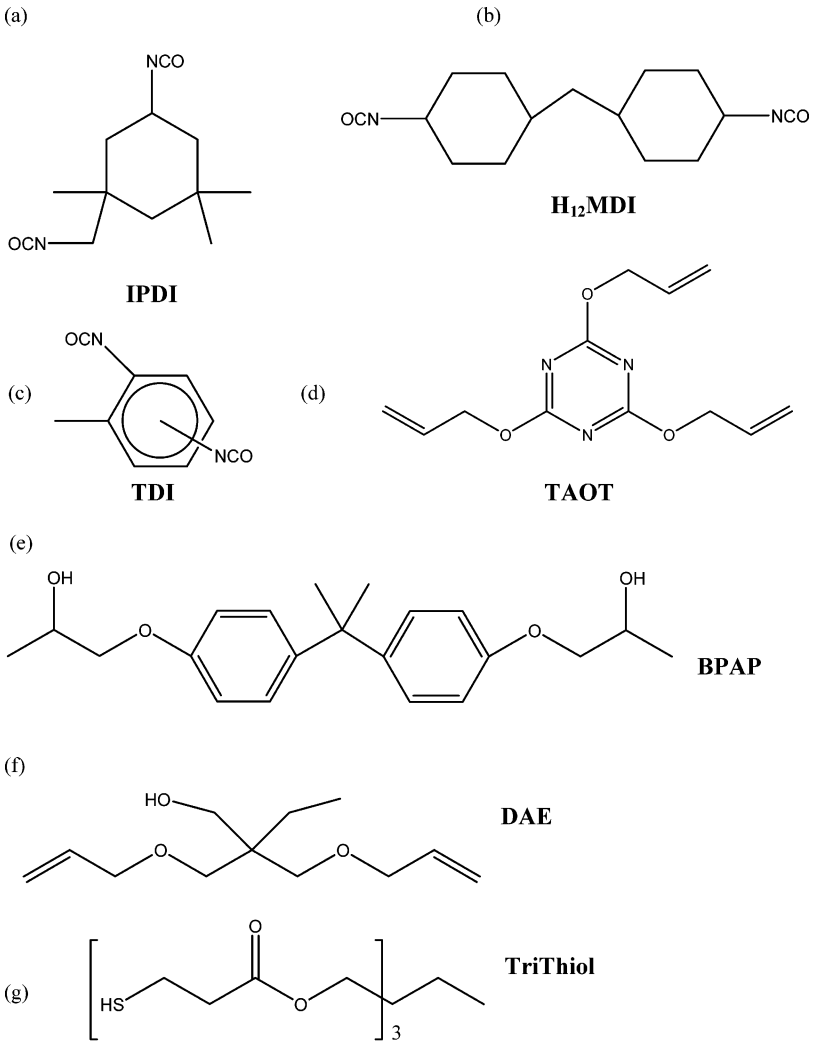

synthesized in order to improve the fracture toughness and high impact resilience of highly cross-linked thiol−ene polymers. In the first set, urethane structures were incorporated into ene monomers by using the condensation reaction of diisocyanates, IPDI, TDI, and H_{12}MDI, with the alcohol group of a diallyl ether to form reactive tetraene monomers. The IPDI-based tetraene is well-known[10] as the ene monomer used for many years in the fabrication of polymer dispersed liquid crystals; however, its physical and mechanical properties in the context of the thiol−ene networks have never been evaluated. In the second set of ene monomers, bisphenol A and urethane structures were integrated by the polyaddition reaction of excess diisocyanates with bisphenol A diol to form reactive intermediates which were then reacted with the alcohol group of the diallyl ether to form a set of reactive tetraene monomers. Photopolymerization reactions of the synthesized ene monomers with trifunctional thiol were monitored by spectroscopic methods, while the mechanical and fracture properties of cured materials were examined over a wide temperature range to assess the temperature dependence of energy absorption upon nondestructive impact and to elucidate the effect of structural features on the glass transition temperature. Thus, both the influence of urethane chemical structure on material properties and the effect of the bisphenol A unit in conjunction with the aromatic and aliphatic urethane structures on polymer mechanical and physical properties have been determined.

Experimental Section

Materials. Trimethylolpropane tris(3-mercaptopropionate) (TriThiol), trimethylolpropane diallyl ether (DAE), isophorone diisocyanate (IPDI), bisphenol A propoxylate (BPAP), triallyloxytriazine, and dibutyltin dilaurate were purchased from Aldrich Chemical Co. 4,4′-Methylenebis(cyclohexyl isocyanate) (H_{12}MDI) and toluene diisocyanate (TDI) were obtained from Bayer. 2,2-Dimethoxy-2-phenylacetophenone (DMPA) was obtained from Ciba Specialty Chemicals. All chemicals (Chart 1) were used as received without further purification.

Synthesis of Monomers. The first set of tetraene monomers (Chart 2) were synthesized by reacting the diisocyanates (IPDI, H_{12}MDI, and TDI) with the hydroxyl functionality of trimethylolpropane diallyl ether. The condensation reactions between trimethylolpropane diallyl ether and diisocyanates (IPDI, H_{12}MDI, and TDI) were in the NCO/OH = 1 stoichiometric ratio. The reactions were carried out in a 250 mL round-bottom flask equipped with a mechanical stirrer and a nitrogen inlet at 55 °C over 24 h. In each case, the diisocyanate was added to the mixture of DAE and dibutyltin dilaurate (0.1 wt % of total mixture). The second set of BPAP-based tetraene monomers (Chart 2) were synthesized by using a 10:9:1 functional group molar mixture of isocyanate to DAE alcohol to BPAP alcohol functional group molar ratio. BPAP,

Chart 2. Chemical Structures of (a) DAE−IPDI−DAE (TAE1), (b) DAE−H_{12}MDI−DAE (TAE2), (c) DAE−TDI−DAE (TAE3), (d) DAE−IPDI−[BPAP−IPDI]$_{n=0,1}$−DAE (TAE4; 90% of $n = 0$, and 10% of $n = 1$), (e) DAE−H_{12}MDI−[BPAP− H_{12}MDI]$_{n=0,1}$−DAE (TAE5; 90% of $n = 0$, and 10% of $n = 1$), and (f) DAE−TDI−[BPAP−TDI]$_{n=0,1}$−DAE (TAE6; 90% of $n = 0$, and 10% of $n = 1$)

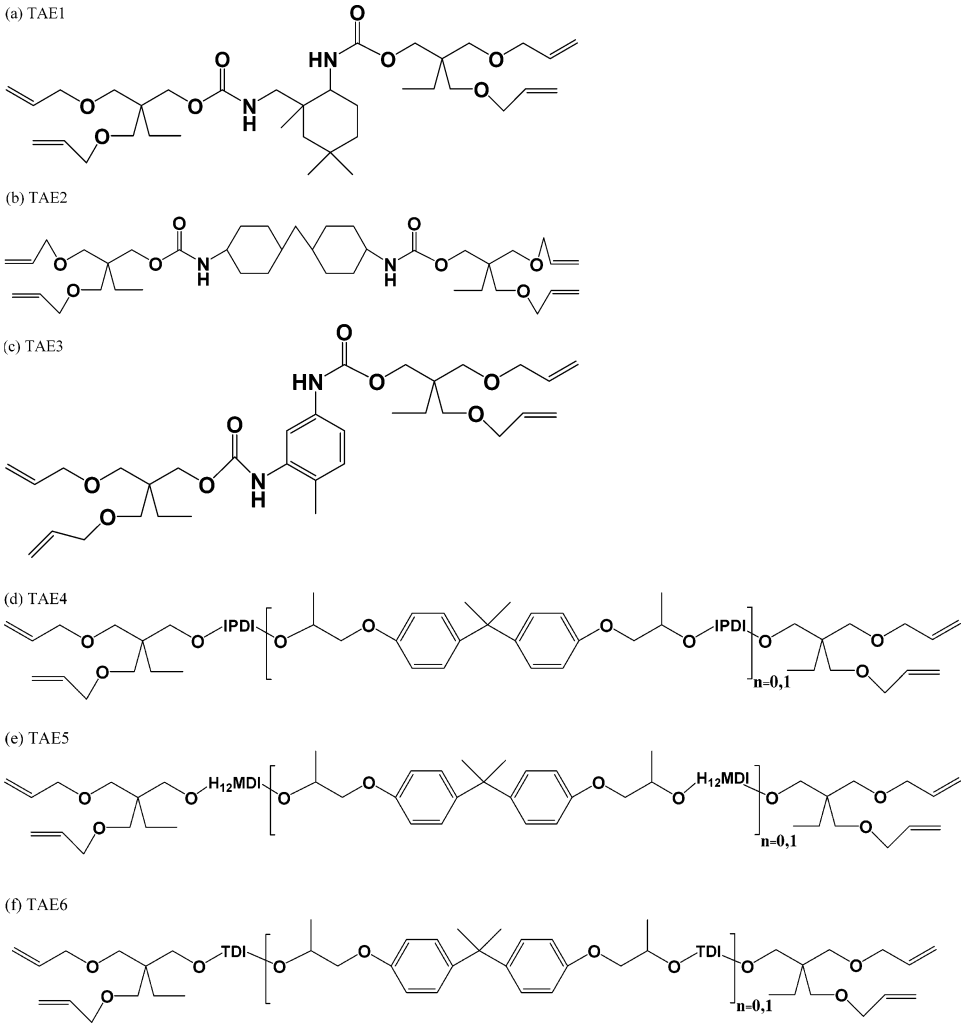

a solid at room temperature, was dissolved in DAE initially and then added to the requisite diisocyanates and allowed to react (45−55 °C). The reactions were monitored with FTIR by following the decrease in the NCO band at 2250 cm^{-1}. The synthesized monomer mixtures, which were mixtures consisting of 90 mol % of the tetraene with no BPAP incorporated and 10 mol % of the tetraene with BPAP incorporated, were used without any further purification. Theoretical molecular weights of the synthesized urethane tetraene monomer mixtures were calculated according to the stoichiometric ratio between diisocyanates and alcohols.

^{13}C and ^{1}H NMR spectra were collected on a Varian 300 MHz NMR in $CDCl_3$ with tetramethylsilane (MTS) as the internal reference. TAE1: ^{1}H NMR (CD_3OD, δ ppm) 5.89 (m, C═CH−CO), 5.22 (q, H_2C═C−CO), 4.72 (bs, NH), 4.52 (m), 4.02 (d, C−CH_2−OCO), 3.94 (d, C═CCH_2−O), 3.32 (s, O−CH_2−C−C_3), 2.93 (bs), 0.8−2.0 (bm, CH). ^{13}C NMR (CD_3OD, δ ppm) 157.07, 135.26, 116.38, 72.21, 70.23, 67.44, 65.33, 54.84, 46.42, 44.48, 42.50, 36.39, 35.04, 31.82, 27.62, 22.89, 7.60.

TAE2: ^{1}H NMR (CD_3OD, δ ppm) 5.89 (m, C═CH−CO), 5.22 (q, H_2C═C−CO), 4.72 (bs, NH), 4.02 (s, C−CH_2−OCO), 3.94 (d, C═CCH_2−O), 3.32 (s, O−CH_2−C−C_3), 0.8−2.0 (bm, CH). ^{13}C NMR (CD_3OD, δ ppm) 155.88, 135.10, 116.26, 72.23, 70.38, 64.99, 47.14, 42.49, 33.42, 32.06, 29.63, 28.08, 22.95, 7.63.

TAE3: ^{1}H NMR (CD_3OD, δ ppm), 7.32, 7.26, 7.08, 6.61, 6.37 (aromatic (TDI) H), 5.88 (m, C═CH−CO), 5.22 (q, H_2C═C−CO), 4.15 (d, C−CH_2−OCO), 3.94 (d, C═CCH_2−O), 3.35 (s, O−CH_2−C−C_3), 2.20, 1.75, 1.45, 0.88, (m, CH). ^{13}C NMR (CD_3OD, δ ppm) 153.87, 135.04, 130.74, 116.43, 72.27, 70.33, 65.92, 42.54, 22.95, 17.04, 7.65.

TAE4: ^{1}H NMR (CD_3OD, δ ppm) 6.81, 7.13 (d, BPAP), 5.89 (m, C═CH−CO), 5.22 (q, H_2C═C−CO), 4.72 (bs, NH), 4.52 (m), 4.02 (d, C−CH_2−OCO), 3.94 (d, C═CCH_2−O), 3.32 (s, O−CH_2−C−C_3), 2.93 (bs), 0.8−2.0 (bm, CH). ^{13}C NMR (CD_3OD, δ ppm) 157.09, 135.09, 127.71, 116.29, 113.91, 72.23, 70.38, 65.33, 54.86, 44.51, 42.51, 36.37, 35.04, 31.84, 27.62, 22.89, 7.62.

TAE5: ^{1}H NMR (CD_3OD, δ ppm) 7.13−6.18 (m, BPAP), 5.89 (m, C═CH−CO), 5.22 (q, H_2C═C−CO), 4.72 (bs, NH), 4.02 (s, C−CH_2−OCO), 3.94 (d, C═CCH_2−O), 3.32 (s, O−CH_2−C−C_3), 0.8−2.0 (bm, CH). ^{13}C NMR (CD_3OD, δ ppm) 155.93, 135.26, 127.75, 116.32, 113.96, 72.28, 70.44, 65.04, 50.39, 47.08, 42.53, 33.60, 32.08, 29.73, 28.14, 22.99, 7.67.

TAE6: ^{1}H NMR (CD_3OD, δ ppm), 6.85, 6.67 (aromatic (BPAP) H), 7.32, 7.26, 7.09, 6.61, 6.36 (aromatic (TDI) H), 5.88 (m, C═CH−CO), 5.22 (q, H_2C═C−CO), 4.15 (d C−CH_2−OCO), 3.94 (d, C═CCH_2−O), 3.35 (s, O−CH_2−C−C_3), 2.19, 1.74, 1.62 (s, CH), 1.47, 0.88 (m, CH). ^{13}C NMR (CD_3OD, δ ppm) 153.96, 136.22, 130.79, 127.79, 116.47, 114.02, 72.31, 70.36, 65.67, 42.56, 22.97, 17.07, 7.68.

Sample Preparation for Testing. The sample formulations were prepared on the basis of equal molar functional groups of tetraene monomer to TriThiol monomer. The photoinitiator, DMPA, with concentration of 1 wt % of total TriThiol and tetraene monomer

was used for thin-film preparation (200 μm), while a lower concentration (0.02 wt %) of DMPA was added to achieve through curing of the thick 1 and 4 mm plates. DMPA was dissolved in the TriThiol and mixed with the synthesized tetraene monomers. Viscosities of the prepolymer mixtures were recorded with a Brookfield, Cap 2000+ viscometer at 25 °C using a 100 rpm spindle speed.

Thick 4 mm plates (impact and thermal dynamic mechanical testing) and 1 mm thick plates (tensile testing) were irradiated with the output of a 305 nm low-pressure mercury lamp (light intensity ~0.1 mW/cm^2) in air followed by exposure to a Fusion light source (see below for description). UV light intensity of the low-pressure lamp at the samples was measured by a calibrated radiometer (International Light IL-1400). Samples were thus first cured (initially intermittently to reduce heat buildup in sample) for a total of 20 min to ensure high conversion of functional groups before passing under the Fusion lamp source (UV Fusion line EPIQ 6000 with D bulb and intensity of 3.146 W/cm^2 at a line speed of 3 m/min: 10 passes—5 front side and 5 back side). As an indication of the uniformity of the various types of 4 mm plates cured by this methodology, the allyl ether ene conversions at the front (1 mm section), middle (1 mm section), and back (1 mm section) of the cured TriThiol-TAE3 plates were determined to be approximately 91%, 90%, and 90% by monitoring the intensity of the allyl ether ene bond at 6120 cm^{-1} with an internal standard at 5790 cm^{-1}. The cured 4 mm TriThiol-TAE6 plate had ~90%, 85%, and 85% allyl ether ene conversions at the top, center, and back, respectively.

Films for evaluating fracture toughness, prepared by drawing down the formulations on a glass plate at a thickness of 200 μm, were cured with a UV Fusion line EPIQ 6000 (D bulb, 3.146 W/cm^2) at a line speed of 3 m/min; each sample was passed under the lamp five times.

Kinetic analyses were conducted with a real-time FTIR (RTIR) in order to confirm conversion vs time plots of thiol and ene monomers. The conversion as a function of irradiation time was recorded on a modified Bruker 88 spectrometer with a 200 W high-pressure mercury−xenon lamp source. In the RTIR measurements, film polymerization was initiated with a light intensity of 1.14 mW/cm^2 at 365 nm. The thiol group conversion was monitored by measuring the area under the peak of the 2570 cm^{-1} band, while the peak at a 3064 cm^{-1} was used for ene double bond conversion calculations in each case.

Thermal and Mechanical Testing. Thermal transitions of thick plates were recorded using a TA Q800 dynamic mechanical analysis (DMA) by heating the samples from −80 to 120 °C at a rate of 2 °C/min and at frequency of 1 Hz in air. DMA was conducted in the cantilever bending mode for specimens with dimensions of 35 mm × 12 mm × 4 mm (L × W × H). Differential scanning calorimetry (TA Q1000) was used to monitor thermal transitions by heating/cooling 5−10 mg samples from −80 to 120 °C at a rate of 10 °C/min under a constant nitrogen flow. TA Q500 thermogravimetric analysis (TGA) was used to determine the thermal degradation temperature by heating 40 mg samples to 550 °C at a rate of 10 °C/min under a continuous nitrogen flow.

The energy absorption measurements were measured by using a Tinius Olsen instrument modified[11] per a configuration used to evaluate nondestructive impact energy absorption properties of thick polymer plates. The instrument analytical procedure was modified to allow accurate values of energy absorption to be calculated from the height of the pendulum upon rebound after striking the sample which consisted of two 4 mm plates pressed together against a steel plate. Typical sample dimensions were 80 mm × 20 mm × 8 mm (L × W × H). The striking edge of the pendulum, complying with ASTM 12.3, was made of hardened steel, tapered to have an included angle of 45° and rounded at the edge to a radius of 3.17 mm. The impact energy was set at 1.13 J. An infrared thermometer (Fisher Scientific) was used to measure the approximate temperature of the samples before the impact absorption tests were conducted.

Tensile properties and fracture toughness measurements were made with a mechanical testing machine, Alliance RT/10. Tensile properties were determined according to ASTM D882, using a 1000 N load cell with a specimen gauge length of 50 mm at a crosshead speed of 25 mm/min. A width−thickness ratio of 8 was used for tensile testing.

Fracture toughness samples were prepared according to ASTM E1820 and ASTM D5045 and tested using a 100 N load cell with a specimen gauge length of 50 mm at a crosshead speed of 25 mm/min in the tension mode. The fracture toughness, K_C, was calculated from eq 1

$$K_C = Y\sigma_F a^{1/2} \tag{1}$$

where the geometry factor Y is $(\sec \pi\, a/W)^{1/2}$, 2a is the notch size, W is the sample width, and σ_F is the tensile strength at failure.[12] The dimensions of the fracture specimens were 100 mm × 50 mm × 0.20 mm (L × W × H), and the ratio $2a/W$ was maintained at a value ca. 0.25 for all samples. A 10 mm notch was placed in the center of the fracture specimens using a sharp blade. In this work, the fracture toughness values were not obtained under plane strain conditions; the results are simply intended to show how K_C varies with urethane structure. A total of 5−10 specimens were used for both tensile and fracture toughness measurements.

Scanning electron microscopy (SEM) was performed on a Quanta 200 SEM in the high-voltage mode. Notched samples fractured in the tensile mode were mounted on the SEM sample holders and sputter-coated with a 5 nm gold layer using a Emitech K550X sputter coater to enhance the image quality.

Results and Discussion

In this study, urethane chemistry was used to synthesize functionalized monomers for thiol−ene reactions. For the comparison of final mechanical properties, the aromatic diisocyanate TDI and aliphatic diisocyanates IPDI and H_{12}MDI (see Chart 1) were reacted with the primary alcohol group of trimethylolpropane diallyl ether (DAE) to form the corresponding urethanes with four double bonds (see TAE1−TAE3 in Chart 2). The products of the solvent-free reaction were controlled by the concentration of the reactants. The molar amount of DAE added was slightly higher than the isocyanate concentration to ensure complete end-capping. Although diisocyanates react with the primary alcohols rapidly in the presence of a catalyst, they can form several different side products, including allophanates, biurets, urea, and isocyanurates.[9] In order to prevent these side products, the reaction of DAE with diisocyanate was kept at lower temperature under a constant nitrogen flow. The glassware was dried carefully before usage to minimize reaction with water. Dibutyltin dilaurate was chosen as the catalyst since it is known to promote urethane formation rather than side products.[9] The complete disappearance of the NCO infrared band at 2250 cm^{-1} was used to monitor the completion of the reaction. In order to analyze the effect of the bisphenol A functionality, 10% of bisphenol A (a dialcohol) was reacted with an excess of each diisocyanate in the presence of DAE under the same reaction conditions to make a second set of tetraenes (TAE4−TAE6) (or $n = 1$ in Chart 2) consisting of mixtures of 90 mol % of TAE1−TAE3 ($n = 0$ in Chart 2) and 10% of the corresponding bisphenol A modified ene. Since the diisocyanates used in this study were isomeric mixtures, the synthesized monomers reflect the formation of isomeric product mixtures. ^{1}H NMR and ^{13}C NMR of each monomer are given in the Experimental Section.

It is well-known that a thiol monomer copolymerizes with an ene monomer, which cannot homopolymerize inherently, in a 1:1 molar functional ratio when exposed to light.[3−7] One of the important parameters characterizing the photopolymerization of a thiol−ene system is thus the functional group conversion as a function of irradiation time. All of the synthesized ene monomers copolymerized with TriThiol efficiently to high

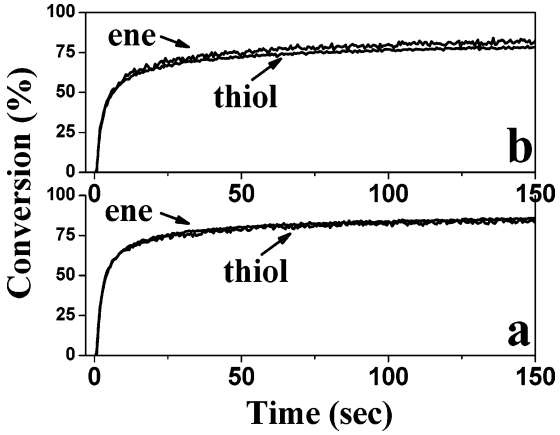

Figure 1. RTIR thiol−urethane ene conversions of 1:1 molar mixtures of (a) TriThiol−TAE3 and (b) TriThiol−TAE6 in air with 1.0 wt % DMPA (light intensity 1.4 mW/cm^2 at 365 nm, high-pressure mercury−xenon lamp source).

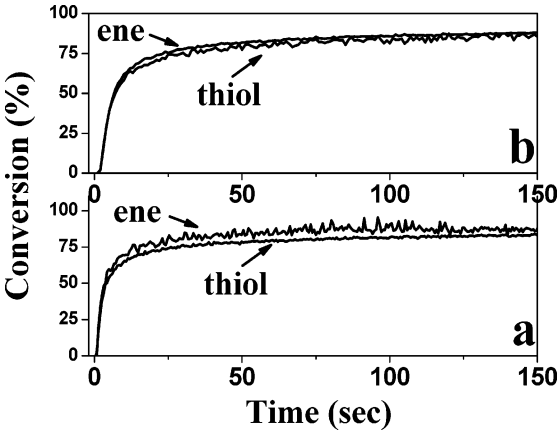

Figure 2. RTIR thiol−urethane ene/diallyl ether conversions of 1:1 molar mixtures of (a) TriThiol−TAE1 and (b) TriThiol−TAE1/10% DAE in air with 1.0 wt % DMPA (light intensity 1.4 mW/cm^2 at 365 nm, high-pressure mercury−xenon lamp source).

conversion. Example RTIR-based conversion vs time plots in Figure 1a,b show that TriThiol copolymerizes with TAE3 and TAE6 very rapidly. As seen in Figure 1b, the incorporation of the BPAP structure with the TDI structure does not alter either the final conversion or the initial rate of the polymerization. Results equivalent to those in Figure 1a,b were obtained for polymerizations of TriThiol with each of the tetraenes in Chart 2.

Because of the presence of strong hydrogen bonding of the urethane groups in the tetraene monomers, they have high viscosities, making them difficult to work with. In order to decrease the viscosities of the thiol−ene mixtures, a reactive diluent ene monomer, trimethylolpropane diallyl ether, which was used in the synthesis of the urethane ene monomers, was added to each of the urethane ene mixtures in varying concentrations, e.g., 4, 8, 10, and 20 mol % of total ene concentration. As is seen by comparison of the results in Figure 2b with the results in Figure 2a, the sample made by replacing 10% of the molar functionality of TAE1 with the DAE diluent does not interfere with the thiol−ene reaction. In fact, the final thiol and ene double bond conversions in Figure 2b reach 90% in a 1:1 copolymerization process. The addition of the DAE was obviously instrumental in enhancing the ultimate conversion (compare parts b and a of Figure 2). Because of the high viscosities of the mixtures, viscosity measurements (25 °C, 100 rpm) of the TriThiol and urethane ene monomer mixtures were

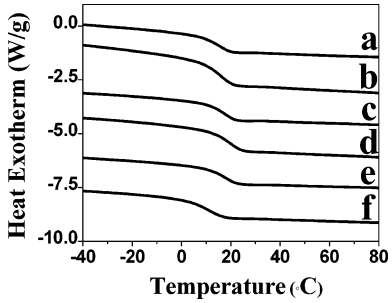

Figure 3. Thermal transitions of TriThiol−urethane tetraene 4 mm plates cured with a 305 nm low-pressure mercury lamp (light intensity 0.1 mW/cm^2) in air: (a) TriThiol−TAE1, (b) TriThiol−TAE4, (c) TriThiol−TAE3, (d) TriThiol−TAE6, (e) TriThiol−TAE2, and (f) TriThiol−TAE5, obtained with DSC, scanning rate of 10 °C/min.

Table 1. Summary of the Viscosity Measurement of TriThiol−Urethane Tetraene Monomers with Varying DAE Concentrations at 25 °C Using a 100 rpm Spindle Speed

formulation	viscosity, Pa·s (at 25 °C, 100 rpm)
TriThiol−90% TAE1/10% DAE	0.8
TriThiol−92% TAE2 /8% DAE	1.9
TriThiol−92% TAE3/8% DAE	1.2
TriThiol−85% TAE4/15% DAE	1.1
TriThiol−92% TAE5/8% DAE	3.9
TriThiol−92% TAE6/8% DAE	2.9

Table 2. Summary of Degradation Temperatures of TriThiol−Urethane Tetraene 4 mm Thick Plates Cured with a 305 nm Low-Pressure Mercury Lamp (Light Intensity 0.1 mW/cm^2) in Air, Obtained with TGA, at a Scan Rate 10 °C/min

formulation	initial DT (°C)	10% weight loss (°C)	50% weight loss (°C)
TriThiol−TAE1	270	310	330
TriThiol−TAE2	260	330	360
TriThiol−TAE3	240	320	350
TriThiol−TAE4	200	320	360
TriThiol−TAE5	260	320	360
TriThiol−TAE6	240	310	350

not determined. However, the addition of small amounts of DAE significantly decreased the viscosities of the thiol−ene mixtures. Example viscosities of TriThiol−urethane ene and DAE mixtures are given in Table 1. Samples containing the BPAP structure have higher viscosities compared to their non-BPAP-containing counterparts. All of the samples were kept at room temperature to prevent premature polymerization prior to UV exposure. The effect of the DAE on the thermal and mechanical properties of the cross-linked network will be discussed in the following paragraphs.

After the photopolymerization of TriThiol with urethane ene monomers, DSC and TGA of the 4 mm thick plates were used to characterize the thermal transitions and thermal stability of the polymer matrices. Figure 3 shows the DSC thermographs of the six different ene monomers copolymerized with TriThiol. Each polymer exhibits a single glass transition temperature (T_g) within the temperature range 10−25 °C. There were no detectable secondary transitions between the −60 and 120 °C scan range. The distinct and narrow glass transitions are indicative of very homogeneous cross-linked networks,[13] which is the one of the hallmark characteristics of thiol−ene polymerizations.[5] Incorporation of a small concentration of BPAP groups into the network does not have any significant effect on the matrix T_g. Multiple DSC scans of the polymers did not result in any shifts in T_g due to post-thermal curing, which is consistent with the high monomer conversion results determined by RTIR. The thermal degradation temperatures listed in Table 2 are in agreement with previously reported[14] thiol−ene degradation

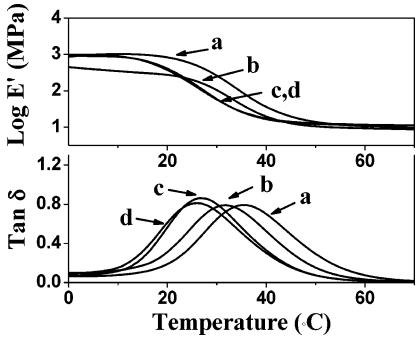

Figure 4. Tan δ_{max} and the storage moduli of TriThiol−TAE2 4 mm plates cured with a 305 nm low-pressure mercury lamp (light intensity 0.1 mW/cm^2) in air with (a) 4% DAE, (b) 8% DAE, (c) 15% DAE, and (d) 20% DAE obtained with DMA, at a scan rate 2 °C/min.

temperatures. All six of the polymers reached 50% weight loss within the temperature range of 330−360 °C, independent of the diisocyanate structure or the incorporation of BPAP. The differential analyses of weight loss curves (not included herein) clearly show overlapping multiple transitions due to the difference in the chemical stability of the BPAP, urethane, and thioether structures.

The thermal mechanical properties of a large number of photopolymerized compositions including monomers TAE1−TAE6 were analyzed by DMA. It was expected that the addition of a low-functionality reactive diluent in the polymer structures would result in a decrease in the tan δ peak maxima in every thiol−urethane ene combination.[13,15] This allowed us to modify the T_g of the six tetraenes (TAE1−TAE-6) by simply adding different concentrations of DAE. Representative example DMA results for TAE2 (tetraene) with DAE (diene) based polymer matrices are given in Figure 4. Increasing the DAE concentration from 4 to 15% decreases the tan δ peak maximum from 35 to 26 °C but does not significantly affect the storage modulus. As was shown by the DSC scans for the plates derived from pure TAE1−TAE6 with TriThiol, the single, narrow tan δ peaks in Figure 4 are indicative of a relatively homogeneous cross-linked network. The high degree of cross-linking via the short connecting linkages do not allow for significant segregation of hard and soft segments within the urethane structures.

A series of mechanical nondestructive impact energy absorption tests (see Experimental Section) typically used to assess energy dissipation of materials used as protective shields were next conducted to compare the performance of a wide selection of photopolymerized TriThiol−ene systems by varying combinations of the tetraenes and DAE. For comparison, the data for two systems, TriThiol−TAE1 and TriThiol−TAE4, without DAE, are also given. The DMA T_gs for the other networks based on TriThiol and tetraene (i.e., TAE2, TAE3, TAE5, and TAE6) will all be around 35−45 °C. A defined impact energy of 1.13 J was imparted to the test specimen with a pendulum to measure the energy absorbed by each thiol−ene network. The absorbed energies measured are of interest for making comparisons of photocured plates under the constraints of the testing configuration. The nondestructive impact experiments were carried on a modified Charpy impact tester. The rectangular shaped, 8 mm thick specimens (two 4 mm plates were pressed together back to back) supported with a steel bar were subjected to a 1.13 J impact energy. Table 3 summarizes the results for the energy absorbed. A previous report[8] indicates that the tan δ_{max} of the test specimen should be near the temperature of impact testing in order to achieve optimum energy absorption by the sample.[16−18] The addition of DAE to the TriThiol−urethane ene mixtures allows one to tune the temperature at tan δ_{max} to optimize energy

Table 3. Summary of tan δ_{max} and Percent Impact Absorption of TriThiol−Urethane Tetraene 4 mm Thick Plates with Varying DAE Concentrations Cured with a 305 nm Low-Pressure Mercury Lamp (Light Intensity 0.1 mW/cm^2) in Air, Obtained with DMA and Impact Testing

formulation	tan δ_{max} (°C)[a]	% impact absorption[b]
TriThiol−TAE1	39	74
TriThiol−90% TAE1/10% DAE	21	91
TriThiol−96 %TAE2/4% DAE	35	83
TriThiol−92% TAE2/8% DAE	31	85.
TriThiol−85% TAE2/15% DAE	26	86
TriThiol−80% TAE2/20% DAE	26	84
TriThiol−96% TAE3/4% DAE	36	83
TriThiol−92% TAE3/8% DAE	27	90
TriThiol−88% TAE3/12% DAE	26	87
TriThiol−TAE4	39	83
TriThiol−85% TAE4/15% DAE	27	89
TriThiol−96% TAE5/4% DAE	33	81
TriThiol−92% TAE5/8% DAE	28	85
TriThiol−88% TAE5/12% DAE	24	88
TriThiol−84% TAE5/16% DAE	24	89
TriThiol−96% TAE6/4% DAE	32	88
TriThiol−92% TAE6/8% DAE	26	89
TriThiol−88% TAE6/12% DAE	26	90
TriThiol−TAOT	23	87

[a] 4 mm thick plates. [b] 8 mm thick plates.

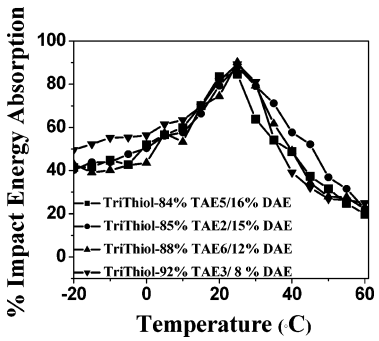

Figure 5. Percent impact energy absorption plot of TriThiol−urethane tetraene of 8 mm thick plates (two 4 mm plates) cured with a 305 nm low-pressure mercury lamp (light intensity 0.1 mW/cm^2) in air as a function of temperature: (■) TriThiol−TAE5−16% DAE, (●) TriThiol−85% TAE2/15% DAE, (▲) TriThiol−88% TAE6/12% DAE, and (▼) TriThiol−92% TAE3/8% DAE (impact force is 1.13 J).

absorption. All of the urethane-containing samples subjected to impact testing exhibited greater than 80% impact energy absorption (Table 3). Adjusting the temperature at tan δ_{max} to 20−30 °C results in impact absorptions from 85 to 90%. Note that, for the samples fabricated from TriThiol and TAE1 vs TriThiol and TAE4 (T_gs at 39 °C) with no added DAE, there is a significant effect of BPAP unit in enhancing energy absorbance at room temperature. This is not seen for the samples with DAE added to lower the T_gs to near room temperature where the impact energy absorption is already inherently high due to a fairly close correlation between the temperature of the tan δ_{max} and the temperature at which the impact occurs. Presumably, a larger BPAP concentration would be needed to give even higher impact energy absorption values. Unfortunately, attempts to incorporate larger concentration of BPAP yielded samples with excessive viscosity that prevented making films, and/or crystallization occurred. The temperature vs % impact energy absorption plot of selected samples given in Figure 5 provides conclusive evidence for a direct correlation between the temperature at tan δ_{max} and the magnitude of the impact energy absorption; i.e., polymer samples with the temperature at tan δ_{max} around 21−27 °C reach near 90% impact absorption at room temperature. For comparison purposes, a

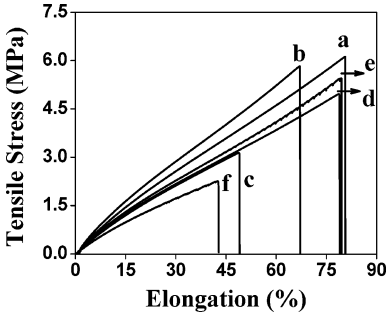

Figure 6. Tensile stress (MPa) vs percent elongation plots of TriThiol−urethane tetraene 1 mm plates cured with a 305 nm low-pressure mercury lamp (light intensity 0.1 mW/cm^2) in air: (a) TriThiol−TAE1, (b) TriThiol−TAE2, (c) TriThiol−TAE3, (d) TriThiol−TAE4, (e) TriThiol−TAE5, and (f) TriThiol−TAE6, obtained with tensile testing machine, at crosshead speed of 25 mm/min.

conventional thiol−ene polymer network formed with TriThiol and TAOT (see Chart 1 for structure) is also included in Table 3. The TriThiol−TAOT-based network has a tan δ_{max} temperature at 23 °C with 87% absorption.

The deformation induced by a tensile force was measured at room temperature for each pure TriThiol−urethane tetraene combination. Thick plates (1 mm) were evaluated by a standard tensile method. We first note that due to the highly cross-linked nature of the thiol−ene photopolymerized samples, stress vs strain curves demonstrated brittle material characteristics; i.e., stress increases linearly with strain without a yield process, and the tensile strength is identical to the breaking strength.[13] As shown in Figure 6, unlike with most highly cross-linked thermoset resins, the elongation at break of the TriThiol−urethane ene samples varies in the range 40−85%. At elongations less than the breaking point, deformation is reversible; the sample recovers to its original shape after the load is removed. These outstanding characteristics of TriThiol−urethane tetraene samples, high elongation with reversible deformation, are attributable to the hydrogen-bonding ability of the urethane structures incorporated into the ene monomers. At room temperature, the polymer formed from 1:1 molar functional ratios of TriThiol and DAE only exhibits 10% elongation before break. The disruption of hydrogen bonds in the urethanethiol−ene-based networks during tensile stretching allows the material to reach high elongation without breaking covalent bonds that would otherwise result in a catastrophic failure.[1,19−23] The block diagram of tensile strength and elongation at break demonstrates the tensile results of the six different urethane tetraene monomers (Figure 7a,b). The samples with aliphatic urethane groups (TAE1 and TAE2) sustain higher tensile stresses with greater elongations than the sample with aromatic urethane groups (TAE3). Samples prepared from the urethane enes containing BPAP structures exhibit lower tensile stresses than their non-BPAP-containing counterparts. Also, the TAE6-containing sample exhibits shorter elongation with incorporation of the BPAP structure (Figure 7b). This might be due to the rigid nature of BPAP groups separating hydrogen-bonding sites within the network. However, this is not the case for TriThiol−TAE5 which has a greater elongation with lower tensile strength at break compared to its TriThiol−TAE2 counterpart. Slight differences in the thermal transitions and the mechanical properties may be attributed to the different isocyanate structures. Previous work[24−26] with a photocurable urethane acrylate exhibited a similar order; i.e., IPDI-based materials exhibited higher modulus and strength at break than TDI-based ones. In order to elucidate the effect of adding reactive diluent DAE on the tensile properties, the samples with compositions TriThiol−

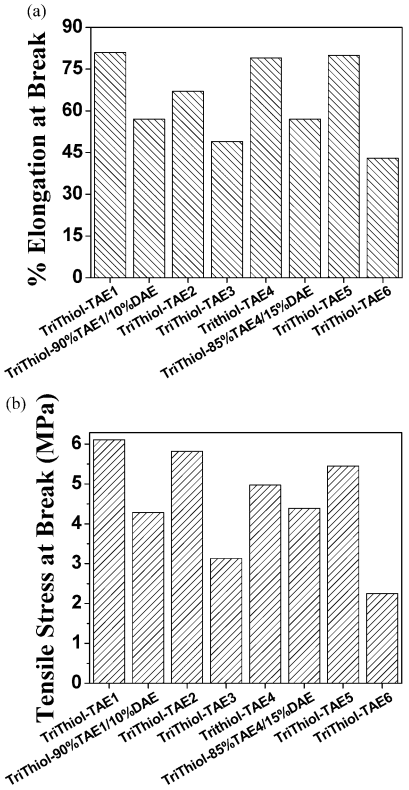

Figure 7. Graphs of (a) percent elongation at break and (b) tensile stress (MPa) at break of TriThiol−urethane tetraene 1 mm thick plates cured with a 305 nm low-pressure mercury lamp (light intensity 0.1 mW/cm^2) in air, obtained with tensile testing machine, at crosshead speed of 25 mm/min.

90% TAE1/10% DAE and TriThiol−85% TAE4/15% DAE were evaluated, and results are also given in Figure 7. The addition of DAE leads to decrease in the stress and elongation at break, while the modulus is increased by 10% for both TAE1 and TAE4 samples, which is consistent with similar diluent effect studies.[15,24−29] The addition of 10% DAE in TAE1 sample decreases the tensile stress at break from 6 to 4 MPa while elongation at break decreases by 24%. Likewise, the incorporation of 15% DAE in the TAE4 formulation decreases elongation at break by 22% whereas tensile stress decreases from 5 to 4.3 MPa. This effect can be explained by the lower T_g of samples with DAE which decreases the tensile properties while improving the modulus.

Next films with predetermined flaw size were subjected to tensile forces in order to measure the fracture toughness of the materials. The resistance of a brittle material to the crack propagation of a flaw is defined as fracture toughness.[12,19,20,23] The fracture strength of a material is a function of several factors including cohesive forces between atoms, such as primary and secondary bonds, chain entanglement, and cross-linked mesh size as well as cross-linking density, free volume, and molecular weight.[12,19,23] The input impact energy is dissipated by both molecular relaxations and bond breakage. Highly cross-linked thermoset polymers such as epoxides and unsaturated polyesters suffer from irreversible bond breakage, leading to catastrophic fracture due to insufficient deformation mechanisms.[20] Fracture toughness of polymers is controlled not only by the elastic deformation at the crack tip but also by plastic deformations. Because of the complexity of these elastic and plastic zone effects on the fracture stress, it is important to eliminate the contribution from plastic deformation which results in brittle fractures. It is known that the fracture stress of highly cross-

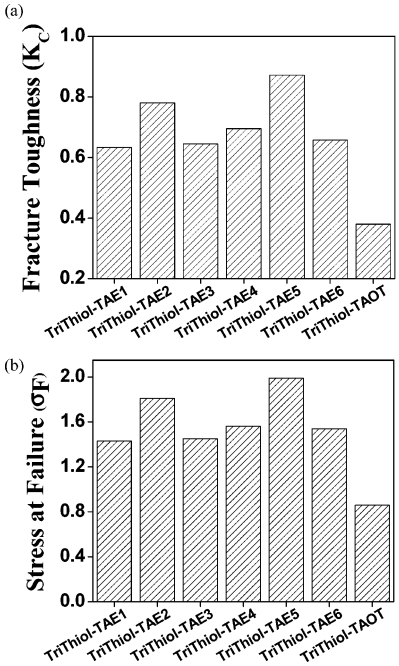

Figure 8. Graphs of (a) fracture toughness (MPa $m^{1/2}$) and (b) tensile stress (MPa) at failure of TriThiol−urethane tetraene notched (200 μm) films cured with a UV Fusion EPIQ 6000 (D bulb 3.146 W/cm^2 at a line speed of 3 m/min), obtained with tensile testing machine, at crosshead speed of 25 mm/min.

Table 4. Summary of the Stress at Failure, Fracture Toughness, and Young Modulus of TriThiol−Urethane Tetraene Notched Films (200 μm) Cured with a UV Fusion EPIQ 6000 (D Bulb 3.146 W/cm^2 at a Line Speed of 3 m/min), Obtained with Tensile Testing Machine at Crosshead Speed of 25 mm/min

formulation	σ_F (MPa)	K_C (MPa·$m^{1/2}$)	Young's modulus (MPa)
TriThiol−TAE1	1.43 ± 0.05	0.63 ± 0.02	34 ± 1
TriThiol−TAE4	1.56 ± 0.02	0.69 ± 0.01	56 ± 4
TriThiol−TAE2	1.81 ± 0.06	0.78 ± 0.02	78 ± 3
TriThiol−TAE5	1.99 ± 0.03	0.87 ± 0.01	84 ± 6
TriThiol−TAE3	1.45 ± 0.03	0.64 ± 0.01	43 ± 2
TriThiol−TAE6	1.54 ± 0.03	0.66 ± 0.01	49 ± 3
TriThiol−TAOT	0.86 ± 0.01	0.38 ± 0.01	22 ± 1

linked thermosets increases with increasing cross-linked density, thus decreasing the plastic flow at the crack tip.[20−22] Additionally, the presence of stress concentrators such as microflaws, voids, corner defects, or any kinds of imperfections within the network structure lead to the nonuniform stress distribution and the formation of hot bonds.[12,19,20,23] The existence of highly stressed bonds causes the failure of the materials under a stress which is less than bond fracture stresses. In this work, thin films were chosen for fracture toughness measurements in order to minimize these stress concentrators. The fracture toughness values of the thin films calculated according to eq 1 are summarized in Table 4. It is noted that the values reported here were obtained in the plane stress fracture toughness region in which the thickness of the specimen is less than the flaw size. According to the results, the fracture toughness and Young's moduli of the TriThiol−urethane tetraene polymers exhibit a similar trend with the TAE5-based films having the highest values for both (Figure 8a,b). For comparison, results for the film formed from a 1:1 molar ratio of TriThiol−TAOT are also included in Table 4. The incorporation of a relatively small amount of BPAP thus improves the fracture toughness of the materials due to the rigid nature of the phenol ring that serve as stress bearing points[9,13,19] (Figure 8a). Owing to the absence

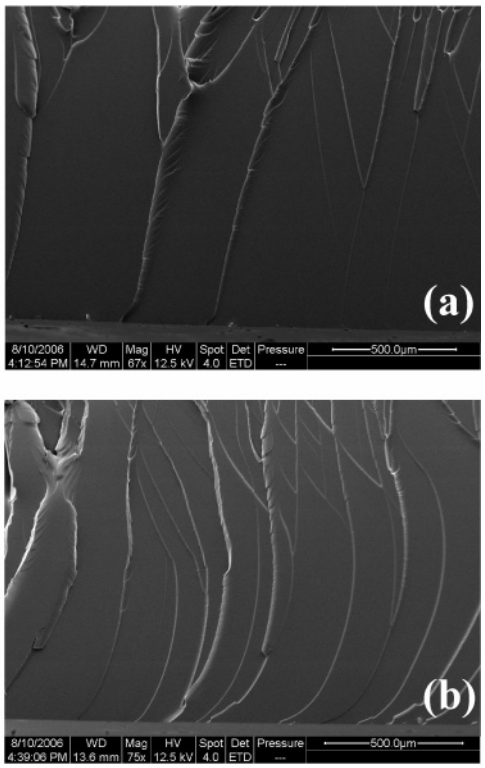

Figure 9. SEM images of fracture surfaces of (a) TriThiol−TAE2 and (b) TriThiol−TAE5. The scale bar is 500 μm.

of other deformation mechanisms, such as secondary relaxations, entanglements, and high molecular weight between cross-links, in these thiol−ene-based thermoset polymers, the incorporation of urethane structures in the network will reduce the stress via a reversible hydrogen bond breaking/re-forming process.[1,19−23] This is presumably the reason for the higher stress values of thiol−urethane ene networks at failure (Figure 8b). The traditional thiol−ene plate made from TriThiol−TAOT, which has a glass transition temperature (23 °C) and comparable impact energy absorption (87%) to thiol−urethane tetraene-based polymers, has 40−60% lower values for fracture toughness and stress at failure than the urethane-containing networks. This clearly shows the higher fracture resistance of urethane-based thiol−ene systems which have higher Young's moduli than the TriThiol−TAOT-based film. For example, the TAE5-based thiol−ene film has a Young's modulus (84 MPa) which is 4 times higher than that of the film formed from TriThiol−TAOT (22 MPa). Also, the fracture toughness and stress at failure values of TriThiol−urethane tetraene polymer networks as shown in Figure 8 perform well compared to reported literature values for epoxy polymers and polyester thermosets (0.6 MPa $m^{1/2}$).[30]

Finally, the scanning electron micrographs of the fractured surfaces of TriThiol−TAE2 and TriThiol−TAE5 are shown in Figure 9. Notched samples were fractured in the tensile mode. All six of the TriThiol−urethane tetraene polymers exhibit similar SEM micrographs. The narrow and continuous fracture paths in the example images in Figure 9a,b are evidence of brittle fracture with rapid crack propagation.[23] Because of the high cross-link density of thiol−ene thermosets, fractures result mostly from elastic deformations. The absence of feathery fracture paths is indicative of a brittle fracture behavior, which is required for proper fracture toughness analysis of polymers.[12,19,23] Fracture surfaces are smooth and shiny due to brittle fracture formation. The SEM images validate linear elastic

fracture formation for these samples and lend credence to calculation of the fracture toughness values presented herein.

Conclusion

In conclusion, this study represents an initial effort to fill the information gap in the literature about the thermal and mechanical characterization of highly cross-linked thiol−ene thermoset polymers. The synthesis of the urethane tetraene monomers was performed in order to integrate the advance mechanical properties of urethane groups into thiol−ene networks. Additionally, bisphenol A structures were incorporated in the ene monomer structure to enhance the fracture toughness and nondestructive impact absorption of the final polymer networks. It has been shown herein that urethane chemistry combined with thiol−ene chemistry allows one to produce by photopolymerization a wide variety of materials with improved mechanical properties. Elongations as high as 80%, and impact absorptions as high as 90%, can be achieved with the proper thiol−urethane tetraene combinations. Fracture toughness of the TriThiol−urethane tetraene polymers are significant and compared favorably to traditional thiol−ene networks and literature values reported for epoxy and polyester thermoset resins. The uniform cross-linked formation of thiol−enes in addition to the strong hydrogen bonding of urethane structures make fracture toughness considerable, which would otherwise be insignificant.

Acknowledgment. This work was supported by the MRSEC Program of the National Science Foundation under Award DMR 0213883 and Fusion UV Systems.

Note Added after ASAP Publication. This article was published ASAP on March 31, 2007. Figure 8a has been modified. The correct version was published on April 17, 2007.

References and Notes

(1) Roffey, C. G. *Photogeneration of Reactive Species for UV Curing*; John Wiley and Sons: New York, 1997.
(2) Dusek, K. In *Developments in Polymerization*; Harvard, R. N., Ed.; Applied Science: London, 1982; Vol. 3, Chapter 4.
(3) Morgan, C. R.; Magnotta, F.; Ketley, A. D. *J. Polym. Sci., Part A* **1977**, *15*, 627−645.
(4) Jacobine, A. F. In *Radiation Curing in Polymer Science and Technology III: Polymerization Mechanisms*; Fouassier, J. D., Rabek, J. F., Eds.; Elsevier: London, 1993; Chapter 7, pp 219−68.
(5) Hoyle, C. E.; Lee, T. Y.; Roper, T. *J. Polym. Sci.* **2004**, *42*, 5301−5338.
(6) Chiou, B.; Khan, S. A. *Macromolecules* **1997**, *30*, 7322−7328.
(7) Cramer, N. B.; O'Brien, A. K.; Bowman, C. N. *J. Polym. Sci., Part A* **2006**, *44*, 2007−2014.
(8) Senyurt, A. F.; Wei, H.; Philips, B.; Cole, M.; Nazarenko, S.; Hoyle, C. E.; Piland, S.; Gould, T. *Macromolecules* **2006**, *39*, 6315−6317.
(9) Oertel, G. *Polyurethane Handbook*; Hanser-Gardner Publications: Cincinnati, 1993.
(10) Smith, G. W. *Mol. Cryst. Liq. Cryst.* **1991**, *196*, 89−102.
(11) Craig, R. G.; Godwin, W. C. *J. Oral Rehab.* **2002**, *29*, 146.
(12) Calliester, W. D. *Material Science and Engineering*; John Wiley and Sons: New York, 1999; Chapter 8.
(13) Nielsen, L. E.; Landel, R. F. *Mechanical Properties of Polymers and Composites*; Marcel Dekker: New York, 1994; Chapter 1, p 4.
(14) Senyurt, A. F.; Wei, H.; Hoyle, C. E. *Macromolecules* **2006**, *39*, 6315−6317.
(15) Nabeth, B.; Gerard, J. F.; Pascault, J. P. *J. Appl. Polym. Sci.* **1996**, *60*, 2113−2123.
(16) Wada, Y.; Kasahara, T. *J. Appl. Polym. Sci.* **1967**, *11*, 1661−1665.
(17) Vincent, P. I. *Polymer* **1974**, *15*, 111−116.
(18) Ochi, M.; Iesako, H.; Nakajima, S. *J. Appl. Polym. Sci., Phys.* **1986**, *24*, 251−261.
(19) Browstow, W.; Corneliussen, R. D. *Failure of Plastics*; Hanser Publishers: New York, 1986; Chapter 2, pp 7−11.
(20) Wool, R. P.; Sun, X. S. *Bio-Based Polymers and Composites*; Elsevier Academic Press: New York, 2005; Chapter 6, pp 150−171.
(21) Lu, J.; Wool, R. P. *J. Appl. Polym. Sci.* **2006**, *99*, 2481−2488.
(22) Lemay, J. D.; Swetlin, B. J.; Kelley, F. N. *ACS Symp. Ser.* **1984**, *243*, 165−183.
(23) Kausch, H. H. *Polymer Fracture*; Springer-Verlag: New York, 1978; Chapters 8−9.
(24) Koshiba, M.; Hwang, K. K. S.; Foley, S. K.; Yarusso, D. Y.; Cooper, S. L. *J. Mater. Sci.* **1982**, *17*, 1447−1458.
(25) Li, C.; Nagarajan, R. M.; Chiang, C. C.; Cooper, S. L. *Polym. Eng. Sci.* **1986**, *26*, 1442−1450.
(26) Chiang, W. Y.; Shu, J. W. *J. Appl. Polym. Sci.* **1988**, *36*, 1889−1907.
(27) Oraby, W.; Walsh, W. K. *J. Appl. Polym. Sci.* **1979**, *23*, 3227−3242.
(28) Oraby, W.; Walsh, W. K. *J. Appl. Polym. Sci.* **1979**, *23*, 3243−3254.
(29) Speckhard, T. A.; Hwang, K. K. S.; Lin, S. B.; Tsay, S. Y.; Koshiba, M.; Ding, Y. S.; Cooper, S. L. *J. Appl. Polym. Sci.* **1985**, *30*, 647−666.
(30) Advanced Materials and Processes. *ASM Int.* **1990**.

MA0626463